

# A New Switched Reluctance Motor Design to Reduce Torque Ripple using Finite Element Fuzzy Optimization

S. R. Mousavi-Aghdam\*, M. R. Feyzi\* and Y. Ebrahimi\*

**Abstract:** This paper presents a new design to reduce torque ripple in Switched Reluctance Motors (SRMs). Although SRM possesses many advantages in terms of motor structure, it suffers from large torque ripple that causes problems such as vibration and acoustic noise. The paper describes new rotor and stator pole shapes with a non-uniform air gap profile to reduce torque ripple while retaining its average value. An optimization using fuzzy strategy is successfully performed after sensitivity analysis. The two dimensional (2-D) finite element method (FEM) results, have demonstrated validity of the proposed new design.

**Keywords:** FEM Analysis, Shape Optimization, Switched Reluctance Motor, Torque Ripple Reduction.

## 1 Introduction

SRM is on the focus of many researchers and it is becoming a proper alternative for conventional motors because of its unique advantages. On the other hand, the torque ripple produced by SRM is an important disadvantage and causes some limitations in its applications. There are two categories in which the torque ripple may be studied and reduced; some methods use control and drive strategies to overcome torque ripple but in some others, motor design is considered for torque ripple reduction. Control and drive strategies may reduce torque ripple, but the intrinsic structure of the motor such as saliency limits their efficiency. Therefore, it is necessary to discuss the geometric design of SRM. Some trends aimed at improving the performance of SRM, have discussed torque ripple reduction in drive and control systems [1]-[3]. Several attempts have been made to optimize the geometric shapes of SRM by designing of the stator pole face with a non-uniform air gap and attached pole shoe to the lateral face of the rotor pole in [4], by designing of a notched tooth rotor to optimize the inductance profile and reduce torque ripple in [5], by deterministic methods to determine design parameters using genetic algorithm in [6], by some soft computing methods such as fuzzy method in [7], and by some new structures of SRM in recent years [8]-[10]. A comprehensive review on the performance improvement

like torque ripple is done by authors in [11]. Although, there are some other papers that study on the motor performance through control methods and drive strategies [12]-[14] but in this study, the focus is on the motor design aspects.

In this paper, a new stator and rotor pole shape with a different air-gap profile is proposed. In the new design, the stator and rotor pole edge is increased near the air gap. In addition, the air gap profile is changed during an unaligned position to an aligned position. The new rotor and stator pole shapes reduce torque ripple with retaining its average value and air gap profiles improve starting torque, as well. The optimal shape of the proposed model is obtained from the 2-D FEM analysis using fuzzy strategy.

## 2 Mathematical Model of SRM

The SRM structure has salient poles on both stator and rotor. Only the stator poles carry windings, and there is no winding or magnetic material on the rotor. The windings on the stator are a particularly simple form, where each two opposite stator pole winding are connected in series to form one phase. Each phase has an ohmic winding resistance and a flux linkage which depends on the excitation current and rotor position  $\theta$ . The most important properties of the SRM are its nonlinear angular positioning parameters and nonlinear magnetic characteristic. An elementary equivalent circuit for the SRM can be derived by neglecting the magnetic hysteresis loss, the mutual inductance between the phases and eddy current losses. The applied voltage to phase 'j' is

Iranian Journal of Electrical & Electronic Engineering, 2012.

Paper first received 10 Feb. 2010 and in revised form 8 Oct. 2011.

\* The Authors are with the Department of Electrical and Computer Engineering, University of Tabriz, Tabriz, Iran.

E-mails: Rmousavi@tabrizu.ac.ir and Feyzi@tabrizu.ac.ir.

$$V_j = R_j i_j + \frac{d\varphi_j(\theta, i_j)}{dt} \quad (1)$$

where  $R_j$  is the resistance and  $\varphi_j$  is the flux linkage of phase 'j' and is obtained as

$$\varphi_j = L_j(\theta, i_j) \cdot i_j \quad (2)$$

where  $L_j$  is the inductance which depends on the rotor position  $\theta$  and the phase current  $i_j$ . Then, the phase voltage is

$$\begin{aligned} V_j &= R_j i_j + \frac{d(L_j(\theta, i_j) \cdot i_j)}{dt} \\ &= R_j i_j + L_j(\theta, i_j) \cdot \frac{di_j}{dt} + \frac{dL_j(\theta, i_j)}{d\theta} \cdot \omega_m i_j \end{aligned} \quad (3)$$

In Eq. (3), the three terms on the right-hand side represent the resistive voltage drop, inductive voltage drop and induced back-emf, respectively. The induced back-emf  $e$  is expressed as

$$e_j = \frac{dL_j(\theta, i_j)}{d\theta} \cdot i_j \cdot \omega_m = k \cdot \omega_m \quad (4)$$

where  $k$  is the back-emf coefficient. The produced torque on the shaft satisfies the following equations

$$T(i, \theta) = \sum_{j=1}^n \left( \frac{\partial W_j}{\partial \theta} \right)_{i_j = \text{cte}} \quad (5)$$

$$W_j(i_j, \theta) = \int_0^{i_j} \varphi_j(i_j, \theta) di_j \quad (6)$$

where  $W_j(i_j, \theta)$  is the co-energy as demonstrated [15].

FEM has been used to precisely calculate the magnetic field. The magnetic vector potential  $A$  determines the magnetic field inside the motor in FEM. It satisfies the nonlinear Poisson's equation

$$\frac{\partial}{\partial x} \left( \gamma \frac{\partial A}{\partial x} \right) + \frac{\partial}{\partial y} \left( \gamma \frac{\partial A}{\partial y} \right) = -J \quad (7)$$

In a 2-D Cartesian coordinate system, where  $\gamma$  is the magnetic reluctivity and  $J$  is the current density vector, flux density  $B$  at each element is obtained from

$$B = \text{curl } A \quad (8)$$

Some other quantities, such as torque, can be calculated from the magnetic vector potential  $A$  in the FEM analysis.

### 3 New SRM Design

An 8/6 SRM configuration was selected for the new design. Needed geometrical parameters of proposed SRM design are shown in Fig. 1. These parameters are summarized in Table 1. The stator pole angle  $B_s$  and the rotor pole angle  $B_r$  are increased with coefficients

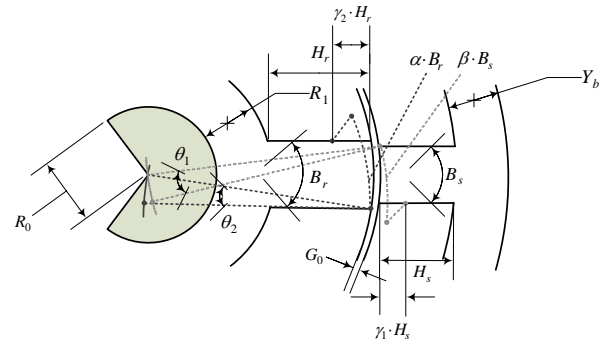


Fig. 1 Geometric parameters of the SRM design

Table 1 Specification of SRM model.

No.	Parameter	Description	Value
1	$G_0$	initial air gap	0.3mm
2	$R_0$	radius of shaft	15mm
3	$R_1$	thickness of outer rotor core	13mm
4	$B_r$	rotor pole angle	23°
5	$B_s$	stator pole angle	21°
6	$H_r$	rotor pole length	19.4mm
7	$H_s$	stator pole length	25.8mm
8	$Y_b$	stator yoke thickness	18.25mm
9	$N$	Number of winding turns	50
10	$\gamma_1$	Stator new pole leg coefficient	0.25
11	$\gamma_2$	Rotor new pole leg coefficient	0.4
12	$W$	Motor Length	0.3m

$\alpha$  and  $\beta$  respectively. The air gap profile is determined by using angular parameters  $\theta_1$  and  $\theta_2$  as shown in Fig. 1. These angles are selected so that the air gap becomes narrower as the rotor pole overlaps with the stator pole. Stator and rotor poles arc extension starting point, are represented by coefficients  $\gamma_1$  and  $\gamma_2$  respectively.

### 4 Optimization Strategy using Fuzzy Functions

Torque ripple reduction with retaining the average value of the torque is the optimization objective in the new design. As mentioned earlier, the evaluation parameters are selected as  $\alpha$ ,  $\beta$  and  $\theta$  for the optimization procedure. The evaluation functions for the torque ripple and average torque are defined as

$$T_m = \frac{1}{n} \sum_{i=1}^n T_i \quad (9)$$

$$T_r = \sum_{i=1}^n |T_m - T_i| \quad (10)$$

where  $T_m$  is the average torque,  $T_i$  is the static torque at the rotor angle  $\theta_i$  and  $T_r$  is the torque ripple. These two functions are combined to form a single objective function by using the fuzzy method. In the fuzzy evaluation,  $\mu_r$  and  $\mu_a$  are defined by  $T_r$  and  $T_m$ , as shown in Fig. 2. As the torque ripple increases, its membership function  $\mu_r$  is decreased. On the other hand, when the average torque increases, its membership function  $\mu_a$  is increased. These membership functions must be as high as possible to reduce torque ripple, and at the same time, increase torque average. Therefore, the objective function is defined as

$$F = -\text{Min}\{\mu_r, \mu_a\} \quad (11)$$

Equation (11) shows that the minimum values of  $\mu_r$  and  $\mu_a$  must be maximized so that the objective function become minimum as Choi, Lee, and Park used in [7].

## 5 FEM Analysis and Results

Because of the highly saturated nature of flux density and the structural complexity of SRM, an analytical model fails to represent the motor accurately. Therefore, a 2-D nonlinear finite-element model is used for electromagnetic analysis. The geometric parameters are designed for a counterclockwise rotating of the rotor, and the torque is calculated for all rotor positions stepped by one degree from 0 up to 30 degrees. A parametric finite-element model of SRM is created and torque characteristics of the motor are extracted as a function of the rotor angle and excitation in each design set. This model facilitates the comparison of the motors with different design variables. In this comparison the turn-on/off angles, the motor speed, and the drive parameters are assumed to remain unchanged.

The sensitivity analysis is a known method to select the most proper parameters of optimization process from a large number of available ones. Motor average torque and torque ripple sensitivity analysis are

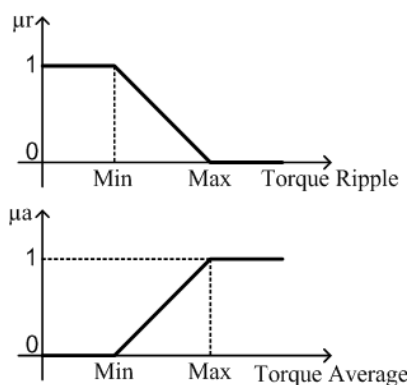


**Fig. 2** Fuzzy membership functions for the torque ripple and torque average.

performed for all six parameters  $\alpha$ ,  $\beta$ ,  $\theta_1$ ,  $\theta_2$ ,  $\gamma_1$  and  $\gamma_2$  in three different levels [16]. The parameter variations along these three levels are summarized in Table 2. It should be noted that the other parameters in Table 1 are general parameters of each conventional SRM, so they are not considered as the sensitivity analysis variables.

Fig. 3(a) shows that the motor normalized average torque has the least sensitivity to  $\gamma_1$  and  $\gamma_2$  relative to other parameters. The same result is obtained for motor normalized torque ripple sensitivity analysis as shown in Fig. 3(b). As an additional result,  $\theta_1$  and  $\theta_2$  both are assumed one parameter because of similar sensitivity and named  $\theta$  after here. Consequently, only  $\alpha$ ,  $\beta$  and  $\theta$  are considered as design parameters in the optimization process and the other parameters are assumed to be constant.

**Table 2** Geometric design parameters for sensitivity analysis

Design Parameter	Level (1)	Level (2)	Level (3)	
1	$\alpha$	1.1	1.2	1.3
2	$\beta$	1.1	1.2	1.3
3	$\gamma_1$	0.2	0.3	0.4
4	$\gamma_2$	0.25	0.375	0.5
5	$\theta_1$	1.1	1.2	1.3
6	$\theta_2$	1.1	1.2	1.3

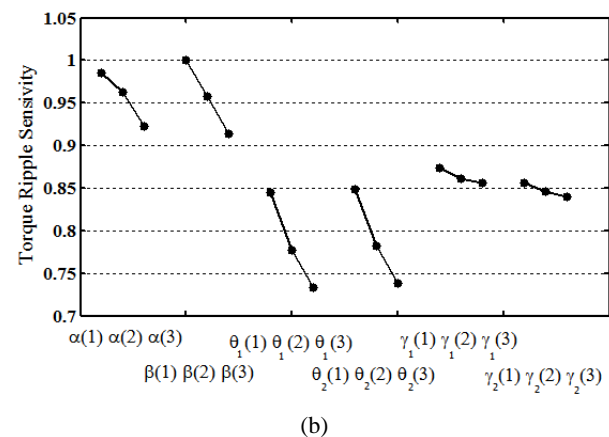
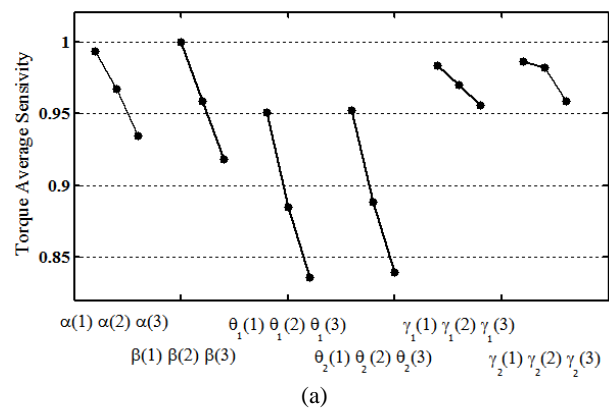
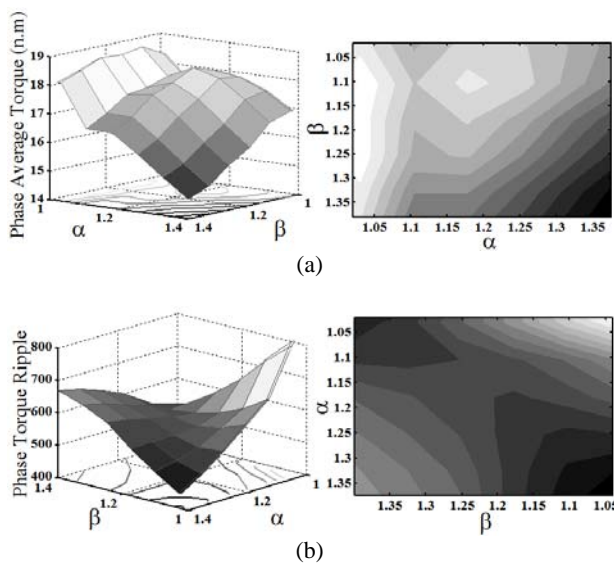


**Fig. 3** Torque average (a) and Torque ripple (b) sensitivity for different levels of parameters.

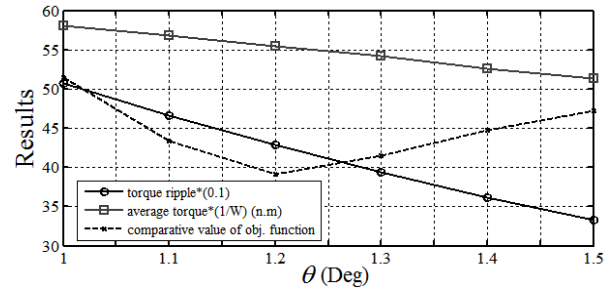
In the first step, the influence of coefficients  $\alpha$  and  $\beta$  on the torque ripple and torque average are investigated where,  $\alpha$  and  $\beta$  are varied from one to 1.4. Fig. 4(a) shows that the average torque is reduced when stator and rotor pole angles increase with the same ratio. Otherwise, the average torque is increased. Fig. 4(a) shows that the average torque has the least value when  $\alpha$  and  $\beta$  are about 1.4.

Fig. 4(b) shows the variation of torque ripple as  $\alpha$  and  $\beta$  are changed from one to 1.4. As shown, torque ripple is increased when  $\alpha$  and  $\beta$  are maximum or minimum simultaneously. It reaches to a minimum when the coefficients  $\alpha$  and  $\beta$  are selected about 1 and 1.4 or vice versa. The optimum values obtained from minimization of the objective function are 1.104 and 1.326 for coefficients  $\alpha$  and  $\beta$ , respectively. In the second step, as mentioned earlier, parameters  $\theta_1$  and  $\theta_2$  become equal named  $\theta$  and torque characteristics are obtained as shown in Fig. 5. The minimum value of  $\theta$  is  $1^\circ$  to make a difference in the motor pole's geometries. As the parameter  $\theta$  is increased, both torque ripple and torque average are decreased. As shown, the optimum value of  $\theta$  obtained from minimization of the objective function is about 1.2.

Closed view of the flux lines of conventional and proposed SRM at fully unaligned position are shown in Fig. 6(a) and (b) respectively. It can be seen that in the conventional motor the fringing flux has the large amount. Fringing flux is known as the main factor of the motor inductance increment at the switching start instant, and its amount varies during rotor rotation. This, results in non-linear phase current and consequently motor torque ripple. A prototype notched rotor pole SRM has been proposed in [5] that produce less torque



**Fig. 4** Response surfaces of phase average torque (a) and phase torque ripple (b) for various values of  $\alpha$  and  $\beta$ .



**Fig. 5** Torque ripple and average profiles and evaluation of objective function for the angle  $\theta$ .

ripple by using fringing flux elimination. Therefore, the new design will help the motor inductance-position profile improvement and torque ripple reduction effectively.

As shown in Fig. 7, in the region around unaligned position the inductance of the proposed motor is more than of the conventional one, but it has a profile similar to the ideal inductance like for an unsaturated motor. Therefore, the current can be increased linearly and torque ripple is reduced consequently.

The phase current rise time limits the phase torque level in the unaligned position adjacency. Around aligned position, in spite of high current level, small inductance derivative causes lack of torque production in the highly saturated motor or in the motor with top flattened inductance profile. As can be seen in Fig. 1 motor rotation is counterclockwise, therefore the proposed design focus is on the phase turn-on angle region. It must be mentioned that in this study, the major attempt is on the new design effects.

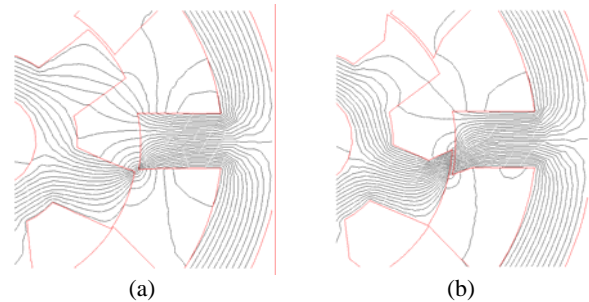


**Fig. 6** Flux lines plot of (a) conventional and (b) proposed SRM.

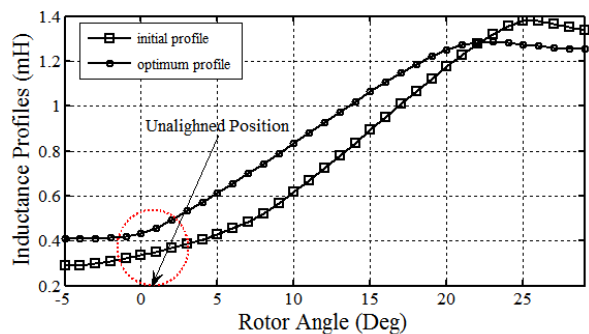


**Fig. 7** Inductance profiles of SRM phase.

Therefore, the FEM analysis is done in the static state and some other effects like magnetizing current can be neglected in this case. Fig. 8 shows the motor phase static torque-position for a defined current level. As shown, the torque variation is small and the average value of torque is acceptable between positions 0 and 20 degree. The phase torque experiences a reduction after position 20 degree, but compared with conventional motor the phase turn-off angle is leaded in proposed motor, so this reduction does not affect the motor total average torque.

Finally, the total static torque of the motor phases, for the optimum and conventional values of design variables, is shown in Fig. 9. After optimization, the motor torque ripple is reduced for the new design, and torque average is remained at the same level.

The comparison between the proposed design and some similar techniques is summarized in Table 3. As shown in the table, torque ripple is efficiently reduced considering the basic torque average in the different design techniques.

**Table 3** Torque characteristics in some different designs.

Design techniques		Torque ripple reduction(%)	Torque average (Nm)
1	Design used in [4]	23	5.5
2	Design used in [5]	4.4	86
3	Proposed Design	34	37

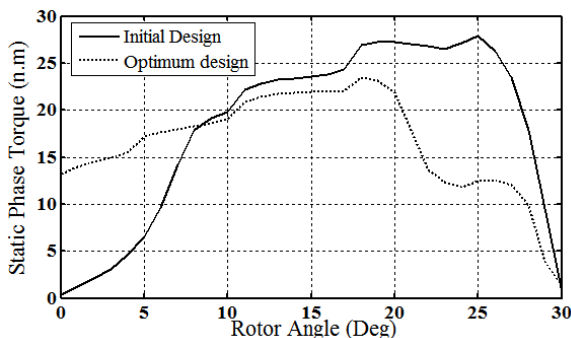


**Fig. 8** Static torques of SRM phase.

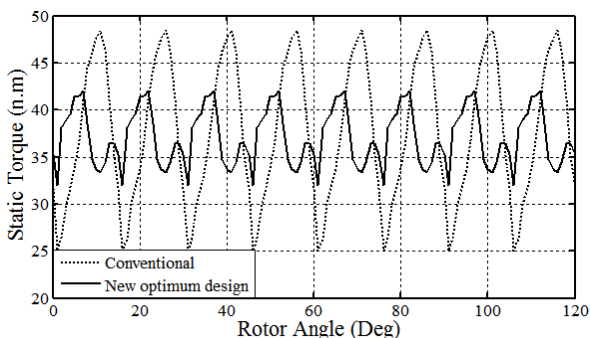


**Fig. 9** Comparison of total static torque waveforms.

Torque ripple reduction in the proposed design has smooth variations in the different motor speeds so that these variations can be neglected for 40 % of changes in the motor basic speed.

## 6 Conclusion

In this paper, a new SRM structure with different rotor and stator pole shapes and a non-uniform air gap profile has been proposed and analyzed. A 2-D FEM analysis using fuzzy method is used to obtain the optimum values of the new design variables. Sensitivity analysis is successfully applied to select the most proper design variables. The effects of each design parameter on torque ripple and torque average were also presented. The new structure has the following advantages over the conventional SRMs.

- The SRM torque ripple is reduced (34% smaller) while retaining the average torque value.
- During unaligned positions, the new structure avoids fringing flux and improves inductance profile.
- In high power applications, the turn-on and off angle can be leaded properly to produce more torque.

## 7 References

- Gobbi R. and Ramar K., "Optimization techniques for a hysteresis current controller to minimize torque ripple in switched reluctance motors", *IET Electric Power Applications*, Vol. 3, No. 5, pp. 453-460, 2009.
- Xue X. D., Cheng K. W. E. and Ho S. L., "Optimization and evaluation of torque-sharing functions for torque ripple minimization in switched reluctance motor drives", *IEEE Transactions on Power Electronics*, Vol. 24, No. 9, pp. 2076-2090, Sep. 2009.
- Inanc N. and Ozbulur V., "Torque ripple minimization of a switched reluctance motor by using continuous sliding mode control technique", *Electric Power System Research (Elsevier)*, Vol. 66, pp. 241-251, 2003.
- Choi Y. K., Yoon H. S. and Koh C. S., "Pole-shape optimization of a switched-reluctance motor for torque ripple reduction", *IEEE Transactions on Magnetics*, Vol. 43, No. 4, pp. 1797-1800, Apr. 2007.
- Lee J. W., Kim H. S., Kwon B. I. and Kim B. T., "New rotor shape design for minimum torque ripple of SRM using FEM", *IEEE Transactions on Magnetics*, Vol. 40, No. 2, pp. 754-757, Mar. 2004.
- Mirzaeian B., Moallem M., Tahani V. and Lucas C., "Multiobjective optimization method based on a genetic algorithm for switched reluctance motor design", *IEEE Transactions on Magnetics*, Vol. 38, No. 3, pp. 1524-1527, May 2002.

- [7] Choi C., Lee D. and Park K., "Fuzzy design of a switched reluctance motor based on the torque profile optimization", *IEEE Transactions on Magnetics*, Vol. 36, No. 5, pp. 3548-3550, Sep. 2000.
- [8] Mao S. and Tsai M., "A novel switched reluctance motor with C-core stators," *IEEE Transactions on Magnetics*, Vol. 41, No. 12, pp. 4413-4420, Dec. 2005.
- [9] Lee C., Krishnan R. and Lobo N. S., "Novel two-phase switched reluctance machine using common-pole E-core structure: concept, analysis, and experimental verification", *IEEE Transactions on Industry Applications*, Vol. 45, No. 2, pp 703-711, Mar./Apr. 2009.
- [10] Oh S. and Krishnan R., "Two-phase SRM with flux-reversal-free stator: concept, analysis, design, and experimental verification", *IEEE Transactions on Industry Applications*, Vol. 43, No. 5, pp 1247-1257, Sep./Oct. 2007.
- [11] Feyzi M. R., Mousavi-Aghdam S. R. and Ebrahimi Y., "A comprehensive review on the performance improvement in switched reluctance motor design", *IEEE CCECE*, May 2011.
- [12] Mousavi-Aghdam S. R., Sharifian M. B. B. and Banaei M. R., "A new method to reduce torque ripple in switched reluctance motor using fuzzy sliding mode", *Iranian Journal of Fuzzy Systems*, In Press (To be published).
- [13] Sedghizadeh S., Lucas C. and Ghafoori Fard H., "Sensorless speed control of switched reluctance motor drive using the binary observer with online flux-linkage estimation", *Iranian Journal of Electrical & Electronic Engineering*, Vol. 5, No. 2, pp. 143-150, Jun. 2009.
- [14] Feyzi M. R. and Ebrahimi Y., "Direct torque control of 5-phase 10/8 switched reluctance motors", *Iranian Journal of Electrical & Electronic Engineering*, Vol. 5, No. 3, pp. 205-214, Sep. 2009.
- [15] Rouhani H., Lucas C., Milasi R. M., and Bahrami M. N., "Fuzzy Sliding Mode Control Applied to Low Noise Switched Reluctance Motor Control", *International Conference on Control and Automation (ICCA)*, pp. 325-329, Jun. 2005.
- [16] Omekanda A. M., "Robust Torque and Torque-per-Inertia Optimization of a Switched Reluctance Motor Using the Taguchi Methods", *IEEE Transactions on Industry Applications*, Vol. 42, No. 2, pp. 473-478, Mar./Apr. 2006.



**Seyed Reza Mousavi Aghdam** was born in Kaleybar, Iran, on April 7, 1987. He received his B.Sc. degree with first class honors in Electrical Power Engineering from Azarbaijan University of Tarbiat Moallem in 2009, Tabriz, and M.Sc. Degree from University of Tabriz with honor in 2011. He is currently working toward the Ph.D. degree in the University of Tabriz. His current research interests include design of electrical machines, electric drives and analysis of special machines.



**Mohammad Reza Feyzi** received his B.Sc. and M.Sc. in 1975 from University of Tabriz in Iran with honor degree. He worked in the same university during 1975 to 1993. He started his Ph.D. work at the University of Adelaide, Australia in 1993. Soon after his graduation, he rejoined to the University of Tabriz. Currently, he is a professor in the same university. His research interests are finite element analysis, design and simulation of electrical machines and transformers.



**Yousef Ebrahimi** received the B.Sc. degree in control engineering from Sahand University of Technology, Tabriz, Iran, in 2001, and the M.Sc. degree in electrical engineering from Tabriz University, Tabriz, Iran, in 2008. Since 2005 he has been with the National Iranian Gas Company (NIGC). He is currently pursuing his Ph.D. in electrical engineering in Tabriz University, Tabriz, Iran. His major research interests are finite element analysis, design and simulation of electrical machines and drives.